Stable two- and three-dimensional geometrically constrained magnetic structures: The action of magnetic fields

V. A. Molyneux, V. V. Osipov, and E. V. Ponizovskaya
Laboratorio de Física de Sistemas Pequeños y Nanotecnología, CSIC, Calle Serrano 144, 28006 Madrid, Spain
(Received 17 December 2001; published 2 May 2002)

We show that equilibrium geometrically constrained domain patterns are two- or three-dimensional magnetic configurations localized around sharp constrictions. Their typical size w depends on both the length d and cross size a of the constriction. When $d<L_0$ the value $w\simeq\min[(2a+d),L_0]$, where L_0 is the conventional wall width. The localized structures undergo small deformation under magnetic fields and at a threshold field they detach from the constriction and magnetization reversal occurs.

DOI: 10.1103/PhysRevB.65.184425 PACS number(s): 75.60.Ch, 75.70.Kw, 75.70.Pa

I. INTRODUCTION

Domain structures determine many properties of real magnetic materials and so there is a great deal of literature devoted to this problem.[1–3] Of particular interest are the domain structures in thin ferromagnetic films,[4–6] which have been intensively investigated during the last decade, primarily because of their giant magnetoresistance.[7] Recent investigations have revealed that magnetoresistance variations of ballistic Ni nanocontacts of diameter 10–100 nm can exceed 700% at room temperature.[8,9] Thus one of the core problems of nanomagnetism and spintronic technology is to understand the properties of magnetic domain patterns in nanoscopic objects and the action of magnetic fields on them.

Estimations show[8,10] that large ballistic magnetoresistance of the Ni nanocontacts can occur when the width of a magnetic domain wall w inside the nanocontacts is less than 1 nm, i.e., when $w\ll L_0$, where L_0 is the width of conventional domain wall in the bulk. In Ref. 11 it was reported that the width of the geometrically constrained wall near a sharp constriction, nanocontact, is essentially given by its length and can be much less than L_0. Recently, the localized magnetic configurations were experimentally investigated in thin Fe films with sharp constrictions.[12]

In this paper we study in more detail magnetic domain structures near a constriction and show that the geometrically constrained one-dimensional (1D) wall studied in Ref. 11 is a nonequilibrium unstable state. The equilibrium patterns are 2D or 3D magnetic configurations localized in the vicinity of the sharp constrictions and their typical width w depends on both the length d and cross size a of the constriction. We also study the dynamics of the formation of the 2D magnetic patterns and the action of a magnetic field on them. Our attention is focused on a thin-film system with a sharp constriction depicted in Fig. 1(a).

II. MAGNETIC STRUCTURES NEAR SHORT CONTACTS

We consider idealized magnetic systems with a sharp constriction in which the easy axis lies along axis y and the magnetization **M** changes as shown in Fig. 1. Let us first, as well as in Ref. 11, neglect the demagnetizing field (corresponding conditions and effect of the demagnetizing fields are discussed below) and write the energy of magnetic domain structures as[1–3]

$$W=\int dV\{A(\boldsymbol{\nabla}\theta)^2+K\sin^2\theta-\mathbf{MH}\}, \tag{1}$$

where θ is the angle between axis y and **M**; A and K are coefficients of exchange interaction and anisotropy; **H** is the external magnetic field, $\mathbf{MH}=M_sH\cos\theta$ when **H** is parallel to the axis y. Notice that we consider the gradients in all possible directions to minimize the magnetic energy W, i.e., x and y for Figs. 1(a) and 1(d); x and z for Fig. 1(b); and x,y, and z for Fig. 1(c). From Eq. (1) it follows the Euler equation for the stationary magnetic structures

$$L^2\nabla^2\theta-1/2\sin 2\theta-h\sin\theta=0. \tag{2}$$

Here $L=\sqrt{A/K}$, $L_0=2L$ is the typical width of the Néel or Bloch domain wall;[1–3] $h=HM_s/2K$, where the homogenous magnetization reversal occurs at $h>1$. We are interested in a solution localized near the constriction and satisfying in extensive systems, $l_1\gg L$ in Fig. 1, the following boundary conditions: $\theta\to 0$ at $y,z\to\pm\infty$ and $x\to\infty$ and $\theta\to\pi$ at $y,z\to\pm\infty$ and $x\to-\infty$.

Let us first analyze the magnetic structures near constrictions when their length d is much less than their cross size a, and this condition, as a rule, is fulfilled in the experiment.[8,9] It would appear natural that typical size of the domain configuration near the constriction $w\ll L$ when $d\ll a\ll L$. Owing to $w\ll L$ the first term of Eq. (2) is much larger than the others for $h<1$ and Eq. (2) is reduced to the Laplace equation $\nabla^2\theta=0$, which does not include any magnetic parameters. This problem for $d\ll a$ is an equivalent, well-known electrostatic task about distribution of a "potential" $\theta(r)$ near a very short contact of width a.[13] For $d\to 0$ this task has exact solution for thin-film systems shown in Figs. 1(a) and 1(b),

$$\theta(x,\zeta)=1/2[\pi+\arg(a^2-x^2-\zeta^2+2iax)], \tag{3}$$

where $\zeta=y$ for Fig. 1(a) and $\zeta=z$ for Fig. 1(b), and an approximate solution for Fig. 1(c) is

$$\theta(r)=\arctan(a/r) \quad \text{for} \quad x>0,$$

$$\theta(r)=\pi+\arctan(a/r) \quad \text{for} \quad x<0, \tag{4}$$

where

$$r=(2a)^{-1}[\sqrt{(a^2+x^2-\rho^2)^2+4x^2\rho^2}-(a^2-x^2-\rho^2)].$$

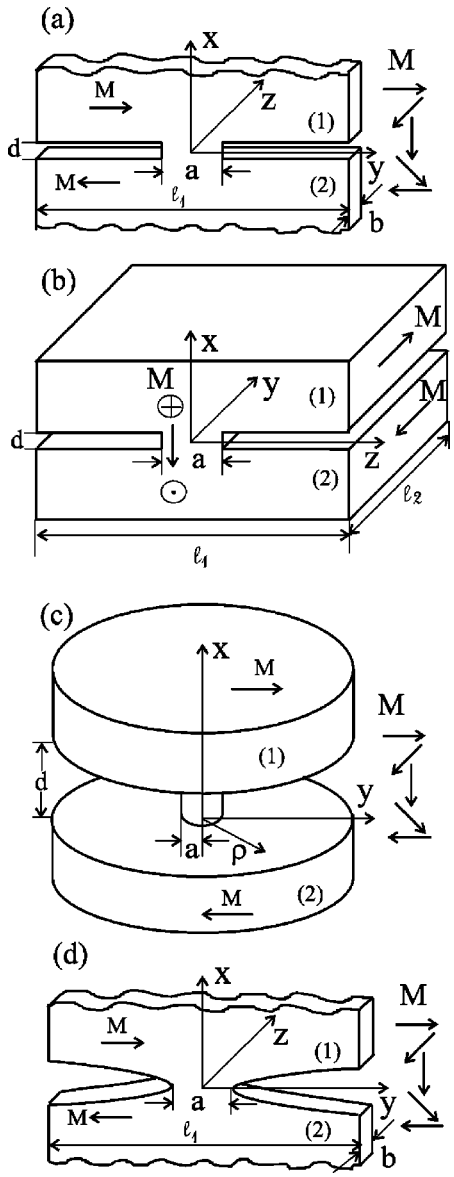

FIG. 1. Schematic representation of magnetic systems with a constriction. The arrows show the direction of the magnetization **M** in the Néel-wall domain structures; θ is the angle between the easy axis y and **M** and ϕ is the angle between the projection of **M** onto the plane (x,z) and the z axis, $\phi=\pi/2$ for the stationary structures under consideration. The values of the cross section of the constriction S_0 are ab, al_2, πa^2, and ab for Figs. 1(a)–1(d), respectively.

From Eqs. (3) and (4) it follows that the constrained domain structures are 2D or 3D magnetic configurations and their typical size w is determined at $d\to 0$ by the cross size of the constriction a; $w\simeq a$ when $d\ll a<L$.

In Ref. 11 it was reported that the width w^* and energy E^* of the geometrically constrained 1D wall do not depend on S_0 in extended enough systems presented in Fig. 1 where S_0 is the cross-section area of the constriction, for example, for the system [Fig. 1(a)] $w^*\simeq d$ and $E^*\simeq \pi^2 AS_0/2d$. From Eqs. (1) and (3) or (4) it follows that the width of the 2D or 3D magnetic structures $w\simeq a>w^*$ and their energy E is less than the energy E^* when $d<a$. This means that the constrained 1D wall is not an equilibrium state at least when $d\ll a$. Moreover, below we show that the 1D wall is an unstable state.

III. FORMATION OF STABLE STRUCTURES

The dynamics and stability of the magnetic domain structures are described by the Landau-Lifshitz equation in which the magnetic structure energy can be written as[1–3]

$$W=\int dV\{A[(\nabla\theta)^2+(\nabla\phi)^2\sin^2\theta] + K\sin^2\theta-\mathbf{MH}-1/2\mathbf{MH}_d\}, \tag{5}$$

where ϕ is the angle between the projection of **M** onto the plane (x,z) and the z axis; $\phi=\pi/2$ for the above considered stationary structures. Additional terms in Eq. (5) as compared with Eq. (1) take into account that in the process of the structure formation $M_z\neq 0$ can arise inducing the demagnetizing field $\mathbf{H}_d=H_z=-4\pi M_z=-4\pi M_s\sin\theta\cos\phi$. Thus, here $\mathbf{MH}_d=-4\pi M_z^2=-4\pi M_s^2\sin^2\theta\cos^2\phi$. This statement is most evident for the thin-film system shown in Fig. 1(a). Using Eq. (5), the Landau-Lifshitz-Gilbert equations for angles θ and ϕ can be written as[1]

$$\partial\theta/\partial t=\alpha^{-1}F_\phi\sin\theta+F_\theta,$$

$$\partial\phi/\partial t\sin\theta=F_\phi\sin\theta-\alpha^{-1}F_\theta, \tag{6}$$

$$F_\theta=2\nabla^2\theta-\sin 2\theta(\nabla\phi)^2-\sin 2\theta - 2h\sin\theta-h_s\sin 2\theta\cos^2\phi, \tag{7}$$

$$F_\phi=2\sin^2\theta\nabla^2\phi+2\sin 2\theta(\nabla\theta\nabla\phi)+h_s\sin^2\theta\sin 2\phi, \tag{8}$$

where $h_s=2\pi M_s^2/K$ and the units of length and time are L and $t_0=(1+\alpha^2)M/\alpha\gamma K$, where γ is the gyromagnetic ratio and α is the Gilbert parameter for viscous damping. We made sure that our main results depend weakly on the value of α, within the typical range $0.03<\alpha<1$, and the boundary conditions when the system size $l_1>4L$. Therefore, for definiteness we have used $\alpha=1$ and $\mathbf{n}\nabla\mathbf{M}=0$ on the boundaries where **n** is the normal to the system surface. We note that the constrained magnetic 1D wall structure found in Ref. 11 satisfies this boundary condition, i.e., is one of the solutions of nonlinear Eq. (2) that also results from Eqs. (6)–(8) for stationary case and $\phi=\pi/2$. Also notice that from Eqs. (3) and (4) it follows that $\nabla\theta\simeq 0$ on the boundaries, where $\theta=0$ or π, at $x=l_1>4L\gg a$. In other words the boundary conditions $\mathbf{n}\nabla\mathbf{M}=0$ and $\theta=0,\pi$ are essentially equivalent for the extensive systems.

Numerical analysis of Eqs. (6)–(8) is carried out with integration steps $\Delta t=10^{-5}-10^{-4}$ and $\Delta x=0.01L-0.04L$ on a net size of 200×200 till 400×400. The steps and system size l_1 are chosen depending upon the parameters d and a so that the system size $l_1\gg w$. Results are presented in Figs. 2–7. Shown in these figures are fragments of size $4L\times 4L$ for the calculated magnetic domain structures in the extensive systems.

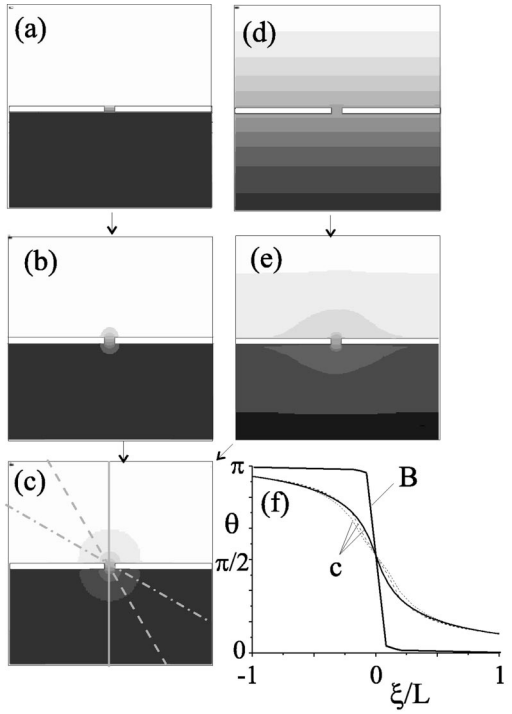

FIG. 2. The formation of a stable geometrically constrained magnetic pattern in a thin-film system [Fig. 1(a)] for $d=0.12L$ and $a=0.2L$, (a) the initial state in the form of the constrained 1D wall found in Ref. 11; (b) an intermediate state at $t=2t_0$; (c) the stationary state at $t>10t_0$; (d) the initial state in the form of the conventional Néel wall; (e) an intermediate state at $t=2t_0$; (f) curves *c* are the distributions of θ along different axes ξ shown in Fig. 2(c) and curve **B** for the 1D constrained wall. Here and below in Figs. 3–6 white and black regions correspond to $\theta=0$ and $\theta=\pi$, respectively.

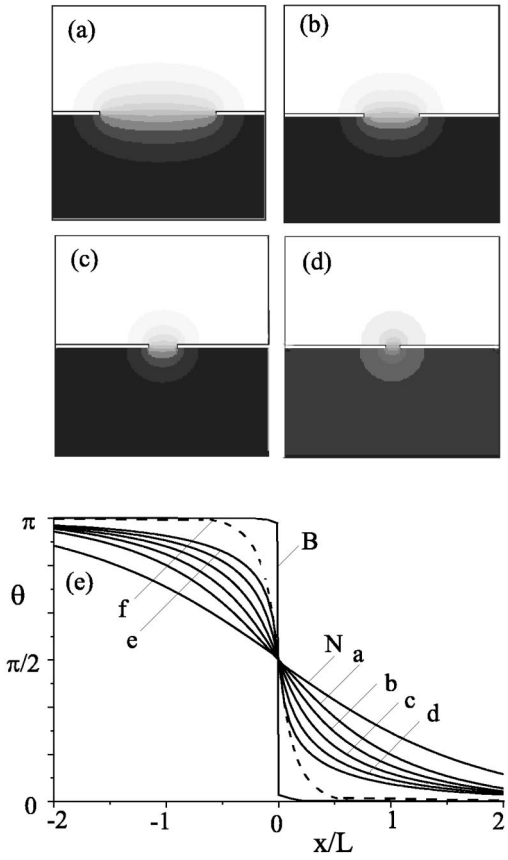

FIG. 3. Stationary magnetic patterns forming in the thin-film system [Fig. 1(a)] in the vicinity of sharp constrictions when their length is much less than the size of cross section of the constriction ($d\ll a$); (a) $a=1.6L$, (b) $a=0.8L$, (c) $a=0.4L$, (d) $a=0.2L$, and (e) distributions of θ along axis *x*, curves *a*–*d* for Figs. 3(a)–(d), curves **N** and **B** for the conventional Néel wall and the constrained 1D wall, and the curves *e* and *f* for the constrained patterns presented in Figs. 5(a) and 5(b), respectively.

The formation of a constrained magnetic structure in the thin-film system [Fig. 1(a)] is shown in Fig. 2 and arising stationary magnetic patterns are presented in Fig. 3 for the case $d\ll a$. We used as the initial states the structure of the constrained 1D wall [Fig. 2(a)] found in Ref. 11 and the Néel-wall structure; $\cosh\theta/2=\exp(x/L)$ [Fig. 2(d)]. One can see that the constrained 1D wall is an unstable state, it extends beyond the region of the constriction [Fig. 2(b)] and a stable 2D configuration is formed around it [Fig. 2(c)]. The Néel wall is also unstable, it sharply shrinks in the regions outside the constriction [Fig. 2(e)] and finally transforms into the same 2D configuration [Fig. 3(c)]. On increasing the calculation time the value $\phi\rightarrow\pi/2$. The shape of the stationary 2D configuration does not depend on the initial state and is determined by the width *a* of the constriction (Fig. 2). As would be expected from Eq. (3) the width of the magnetic configurations $w\simeq a$ when $a<L$ and $w\simeq L$ when $a>L$. In the case $d\ll a$ the calculation distributions $\theta(\xi)$ coincide accurately enough with the $\theta(\xi)$ given by Eq. (3) and weakly depend on the angle between the axis *x* and an axis ξ crossing the constriction center [Fig. 2(f)]. Such type of symmetrical configurations were recently experimentally found in thin-film magnetic systems near sharp constrictions.[12]

The calculations show that the magnetic configuration is localized increasingly inside the constriction with extension of its length *d* (Fig. 4) and width w_0 where θ changes from $\pi/4$ to $3\pi/4$ at $x=0$ along the axis *x* normal to the constriction cross can be approximated as

$$w_0=2L(a+d/2)(L+a+d)^{-1}, \tag{9}$$

with an accuracy of about 20%. In particular, $w_0=3d$ when $a=d\ll L$, see the curve *e* in Fig. 3(e) for $a=d=0.1$.

All the above results relate to the thin-film systems with a sharp constriction presented in Figs. 1(a) and 1(b). We found that they also describe roughly the properties of the magnetic patterns in the system shown in Fig. 1(c). However, in such cylindrically symmetrical systems the magnetic configuration is more localized than in the thin-film systems. Compare Figs. 5(a) with 5(b) and curve *e* with curve *f* presented in Fig. 3(g).

We emphasize that *w* for smooth constriction [Fig. 1(d)] naturally exceeds *w* for the short constriction [Fig. 1(a)]. For example, when $S(x)=ab(1+x^2/d^2)$, the model II in Ref. 11, the magnetic configuration and its width *w* for $d=0.1$ and $a=0.2$ [Fig. 5(c)] coincide approximately with those

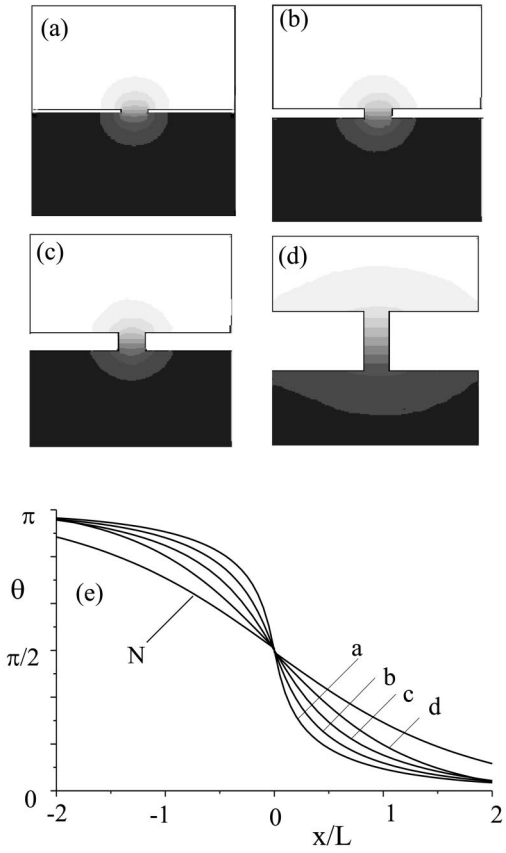

FIG. 4. Stationary magnetic patterns in the thin-film system in the vicinity of sharp constriction for different lengths d at $a=0.4L$; (a) $d=0.04L$, (b) $d=0.2L$, (c) $d=0.4L$, (d) $d=1.2L$; (e) distributions of θ along axis x, the curves $a-d$ for Figs. 4(a)–(d), respectively, and curve **N** for the conventional Néel wall.

presented in Fig. 4(b) for the system with a sharp constriction having substantially larger sizes with $d=0.4$ and $a=0.4$.

IV. THE ACTION OF EXTERNAL MAGNETIC FIELDS

We have emphasized above that the term $h\sin\theta$ in Eq. (2) describing the action of external magnetic fields on the constrained domain structures is small for $h<1$ when their width $w\ll L$. Numerical analysis of Eqs. (6)–(8) shows that, indeed, such strong localized structures are deformed weakly at $h<1$ [Figs. 6(a) and 6(b)] and shift slightly in the region where $\theta=\pi$ for $h>0$. We remind that the homogenous magnetization reversal occurs at $h>1$. The deformation increases with d and a (Fig. 6). For not very small d and a there is a threshold field $h=h_c<1$ such that the constrained structure detaches from the constriction and at $h>0$ the system transforms into a homogeneous state with $\theta=0$. This process is presented in Fig. 7. The calculations show that the value $h_c\simeq 2d/(a+d)$ for $L>d>0.04L$ (see also the caption to Fig. 6).

V. THE INFLUENCE OF DEMAGNETIZING FIELD

Let us now estimate the magnetostatic energy. It is well known[2,3] that in uniaxial ferromagnetic thin films in which

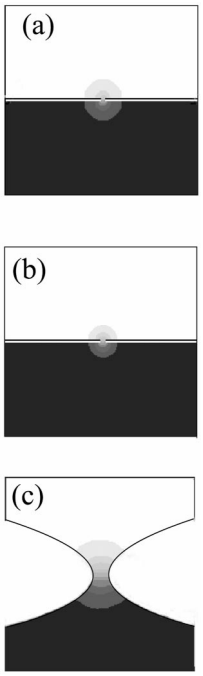

FIG. 5. Stationary magnetic patterns forming in the vicinity of constrictions in the different systems; (a) in the systems shown in Figs. 1(a)–(b) with $a=0.1L$ and $d=0.1L$, (b) in the cylindrical symmetry system shown in Fig. 1(c) with $a=0.1L$ and $\rho=0.1L$, and (c) in the thin-film system shown in Fig. 1(d) with $d=0.1L$ and $a=0.2L$. The curves e and f in Fig. 3(e) and curve d in Fig. 4(e) show the distributions of θ along axis x for Figs. 5(a)–(c), respectively.

the easy axis y lies in the film plane [Fig. 1(a)] the Néel-wall structure is realized and in this case the total magnetic charge is equal to zero and surface magnetic charges do not arise. Therefore, the Néel-wall energy is less than that of the Bloch domain wall. On the other hand, the demagnetizing factor for the Néel structure in the thin films is very small, $N\simeq b/(w+b)$, when the film thickness $b\ll w$.[2,3] Therefore, the energy of the demagnetizing field is, as a rule, a negligible component of the Néel-wall energy in very thin films.[2] We emphasize that this statement is valid to a greater extent for the constrained magnetic structures localized in a region of size $w\ll L$ as the density of their exchange interaction energy is much more than those for the Néel-wall, i.e., $A(\nabla\theta)^2\simeq A(\pi/w)^2\gg A(\pi/L)^2$. Indeed, substituting Eq. (3) into Eq. (1) we find that the exchange interaction energy $E_{ex}\simeq\pi^2 Ab/2$. At the same time the magnetostatic energy is approximately $E_{ms}\simeq\pi M_s^2 w^2 bN\simeq\pi M_s^2 ab^2$. Thus the condition of neglect of the demagnetizing field, $E_{ms}<E_{ex}$, is valid when $ab<(\pi\lambda)^2$ where $\lambda=(A/2\pi M_s^2)^{1/2}$ is the magnetic exchange length. For the typical ferromagnets $\lambda\simeq 3-15$ nm, e.g., for Ni $\lambda\simeq 5$ nm and for permalloy $\lambda\simeq 14$ nm. Thus for the thin-film system [Fig. 1(a)] with thickness of 5 nm $ab<(\pi\lambda)^2$ when $a<20-450$ nm. The same estimation is approximately correct for the thin-film system shown in Fig. 1(d). For the system presented in Fig. 1(b) the magnetization **M** outside the domain structure has only M_y component and we can neglect the magnetic charges on the surfaces $y=0$

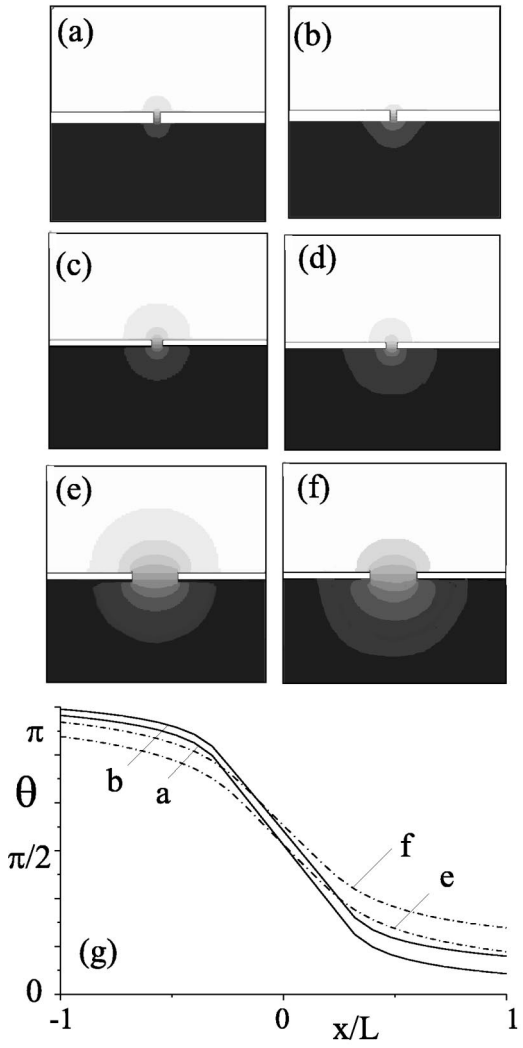

FIG. 6. Deformation of constrained magnetic patterns in the thin-film system under the action of external magnetic field directed along the easy axis *y*. (a), (c), and (e)—stationary states for $h=0$; (b), (d), and (f)—stationary states for $h\neq 0$. (a) $d=0.2L$ and $a=0.12L$, (b) $d=0.2L$, $a=0.12L$, and $h=0.7$ (threshold field $h_c>1$); (c) $d=0.12L$ and $a=0.2L$, (d) $d=0.12L$, $a=0.2L$, and $h=0.5$ ($h_c\simeq 0.7$); (e) $d=0.12L$ and $a=0.8L$, (f) $d=0.12L$, $a=0.8L$, and $h=0.2$ ($h_c\simeq 0.3$); (g) distributions of θ along axis *x*, curves *a*, *b*, *e*, and *f* show $\theta(x)$ for Figs. 6(a), 6(b), 6(e), and 6(f), respectively.

and $y=l_2$ when $l_2\gg L$. Therefore, the total magnetic charge is also equal to zero and the magnetostatic energy $E_{ms}\approx\pi M_s^2 w^2 l_2\simeq\pi M_s^2 a^2 l_2$ when $d<a\simeq w<L$. In this case the exchange interaction energy $E_{ex}\simeq\pi^2 A l_2/2$ and so $E_{ms}<E_{ex}$ when $a<\pi\lambda\simeq 10-50$ nm. The same estimation is approximately correct for the system shown in Fig. 1(c) when **M** outside the domain structure also has the M_y component only.

To estimate the effect of the demagnetizing field on the constrained magnetic structures in the thin-film systems we have used the OOMMF package[14] and also an iteration method. From Maxwell equations

$$\nabla(\mathbf{H}_d+4\pi\mathbf{M})=0,\quad \nabla\times\mathbf{H}_d=0, \tag{10}$$

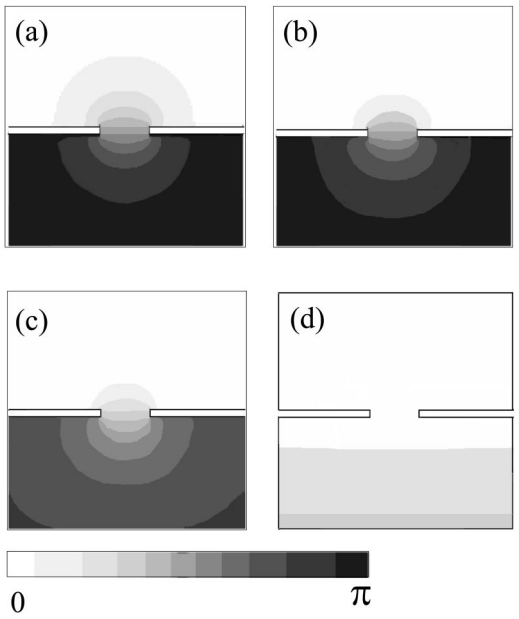

FIG. 7. Dynamics of magnetization reversal under the action of a magnetic field $h=0.5$ in the thin-film system for constriction with $d=0.12L$ and $a=0.8L$; (a) the initial stationary state for $h=0$; (b–d) intermediate states at $t=5t_0$, $t=10t_0$, and $t=15t_0$; the final state with $\theta=0$, white color, is formed for time $t>20t_0$.

it follows that

$$Q\Delta h_{d\xi}=-\partial/\partial\xi(\nabla\mathbf{m}), \tag{11}$$

where $\xi=x,y,z$; $h_{d\xi}=H_{d\xi}M_s/2K$; $\mathbf{m}=\mathbf{M}/M_s=\mathbf{i}\sin\theta\sin\phi+\mathbf{j}\cos\theta+\mathbf{k}\sin\theta\cos\phi$; and $Q=K/2\pi M_s^2$. We substituted the values of $\theta(x,y)$ and $\phi=\pi/2$ calculated above for stationary magnetic structure at $\mathbf{H}_d=0$ into Eq. (11) and found $h_{d\xi}(x,y,z)$. We then used these numerical values for $h_{d\xi}$ in the Landau-Lifshitz-Gilbert equations for angles θ and ϕ. Next we substituted the calculated values of $\theta(x,y)$ and $\phi(x,y)$ into Eq. (11) and found $h_{d\xi}(x,y,z)$ and then new values of angles θ and ϕ. In this way we have estimated the action of the demagnetizing field $\mathbf{H}_d$. We found that in Co films for which $Q\simeq 0.1-0.3$ this action is relatively weak for the sharp constriction shown in Fig. 1(a) when $a<0.3L$ and $d<0.3L$. The stationary form of the constrained structures slightly shrinks and changes significantly only near the corner boundaries of the constriction, i.e., it becomes smoother.

Thus we showed that neglect of the demagnetizing field is valid for the thin-film systems with the magnetic exchange length $\lambda\geqslant 3$ nm at least, but it can limit the correctness of our calculations for the cylindrical symmetry system shown in Fig. 1(c). However, we notice that magnetic configurations near nanocontact between two cylindrical bars with easy axis along the cylinder axis were studied in a recent paper.[15] The authors of Ref. 15 take into account the demagnetizing field and emphasize that the typical scale of the magnetic configurations is proportional to the cross size of the nanocontact.

VI. CONCLUSION

From our calculations we can stress the following conclusions:

(1) The typical width w of the equilibrium geometrically constrained magnetic structures is a function of both the constriction width a and length d. The results of 1D approach used in Ref. 11 are approximately valid only when $a \ll d$.

(2) When $d \ll a < L$ the width $w \simeq 2a$ and the distributions of the magnetization, the angle θ, depends weakly on the angle between the axis x (Fig. 1) and any arbitrary axis ξ crossing the constriction center. Such symmetrical configurations were recently found experimentally in thin-film magnetic systems near sharp constrictions.[12]

(3) The width $w \ll L$ only when both d and a are much smaller than L, i.e., $w \simeq 2a + d$. In this case the action of an external magnetic field on such strong, constrained magnetic structures near the sharp constrictions is very weak.

(4) When $d < a \simeq L$ the constrained magnetic structures determine the process of the magnetization reversal in systems with the constrictions and value of the coercive field.

(5) The weak, constrained magnetic structures near smooth constrictions are very sensitive to the external magnetic field (see also Ref. 16).

(6) The experiments with nanocontacts $10-50$ nm in diameter[9] showing ballistic magnetoresistance (BMR) up to 700% cannot be explained on the basis of the idea of the constrained magnetic wall because in this case the wall width exceeds 10 nm.

The large BMR observed can be explained by wall scattering only when the wall width is smaller than 1 nm.[8,10] To explain such large BMR in $10-50$ nm Ni nanocontacts we have to assume that a very thin dead layer of thickness ~ 1 nm arises accidentally inside the nanocontact[9,17,18] during the electrodeposition growing process (see, for example, Ref. 19). The nanocontact *per se* can be such a dead layer and, most likely, its thickness is of atomic dimension. The authors of Refs. 8 and 9 observed switching of the nanocontact resistance and increase of the magnetoresistance under nanocontact current pulses and assumed that these effects were due to reconstruction of the magnetization configuration in the vicinity of the nanocontact under the action of the magnetic fields. Such local configurations are closed domains on the surface of the wires. They can be roughly considered as domain structures in thin films that constrict and cross at the nanocontact region. We showed in Ref. 17 that the domain wall is attracted to the nanocontact by the action of the magnetic field induced by nanocontact current pulses. The large nanocontact magnetoresistance can be determined by a shift of the domain wall under the action of external magnetic field and the relative rotation of the magnetization between the Ni layers separated by the nanocontact dead layer.[16]

ACKNOWLEDGMENTS

This work has been supported by the EU IST-2000-2001 project. V.V.O. was supported by the Spanish Sabbatical Program and E.V.P. by the financial support of NATO. We also thank N. García, J. A. Rausell Colom, and C. B. Muratov for helpful remarks.

[1] A. P. Malozemoff and J. C. Slonczewski, *Magnetic Domain Walls in Bubble Materials* (Academic Press, New York, 1979).

[2] A. Aharoni, *Introduction to the Theory of Ferromagnetism* (Oxford University Press, New York, 1998).

[3] A. Hubert and R. Schafer, *Magnetic Domains* (Springer-Verlag, Berlin, 1998).

[4] M. Speckmann, H. P. Oepen, and H. Ibach, Phys. Rev. Lett. **75**, 2035 (1995); A. Berger and H. P. Oepen, Phys. Rev. B **45**, 12 596 (1992); R. Jansen, M. Speckmann, and H. P. Oepen *et al.*, J. Magn. Magn. Mater. **165**, 258 (1997).

[5] R. Allenspach and A. Bischof, Phys. Rev. Lett. **69**, 3385 (1992); R. Allenspach, M. Stampanoni, and A. Bischof, *ibid.* **65**, 3344 (1990).

[6] W. H. Rippard and R. A. Buhrman, J. Appl. Phys. **87**, 6490 (2000); B. Heinrich and J. F. Cochran, Adv. Phys. **42**, 523 (1993).

[7] *Ultrathin Magnetic Structures*, edited by B. Heinrich and J. A. C. Bland (Springer, Berlin, 1994); T. Miyazaki and N. Tezuka, J. Magn. Magn. Mater. **139**, L231 (1995); J. S. Moodera *et al.*, Phys. Rev. Lett. **74**, 3273 (1995).

[8] G. Tatara, Y.-W. Zhao, M. Muñoz, and N. García, Phys. Rev. Lett. **83**, 2030 (1999); N. García, M. Muñoz, and Y.-W. Zhao, *ibid.* **82**, 2923 (1999).

[9] N. García, H. Rohrer, I. G. Saveliev, and Y.-W. Zhao, Phys. Rev. Lett. **85**, 3053 (2000); N. García, I. G. Saveliev, Y.-W. Zhao, and A. Zlatkine, J. Magn. Magn. Mater. **214**, 7 (2000); N. García, M. Muñoz, G. G. Qian, H. Rohrer, I. G. Saveliev, and Y.-W. Zhao, Appl. Phys. Lett. **79**, 4550 (2001).

[10] G. G. Cabrera and L. M. Falicov, Phys. Status Solidi B **61**, 539 (1974); G. Mathon *et al.*, in Proceedings of the International Conference on Magnetism, Brazil, 2000 (unpublished).

[11] P. Bruno, Phys. Rev. Lett. **83**, 2425 (1999).

[12] I. V. Roshchin, J. Yu, A. D. Kent, G. W. Stupian, and M. S. Leung, IEEE Trans. Magn. **37**, 2101 (2001).

[13] J. C. Maxwell, *A Treatise on Electricity and Magnetism* (Dover Press, New York, 1891); G. Wexler, Proc. Phys. Soc. Jpn. **89**, 927 (1966).

[14] M. J. Donahue and D. G. Porter, OOMMF User's Guide, Version 1.0 (National Institute of Standards and Technology, Gaithersburg, MD, 1999), http://math.nist.gov/oommf/

[15] L. L. Savchenko, A. K. Zvezdin, A. F. Popkov, and K. A. Zvezdin, Phys. Solid State **43**, 1509 (2001).

[16] N. García, V. V. Osipov, and E. V. Ponizovskaya, Phys. Rev. B **64**, 184412 (2001).

[17] V. V. Osipov, E. V. Ponizovskaya, and N. García, Appl. Phys. Lett. **79**, 2222 (2001).

[18] N. Gorera *et al.*, in Proceedings of the MML'01 Conference, Aachen, 2001 (unpublished).

[19] J.-G. Zhu and H. N. Bertram, J. Appl. Phys. **63**, 3248 (1988).